Journal of Sound and Vibration (2000) **235**(2), 317–340
doi:10.1006/jsvi.2000.2918, available online at http://www.idealibrary.com on IDEAL®

FREE VIBRATION OF SKEW SANDWICH PLATES WITH LAMINATED FACINGS

C. M. Wang, K. K. Ang and L. Yang

Department of Civil Engineering, The National University of Singapore, 10 Kent Ridge Crescent, Singapore 119260, Singapore

AND

E. Watanabe

Department of Civil Engineering, Kyoto University, Kyoto, Japan

(*Received* 8 *May* 1999, *and in final form* 22 *February* 2000)

This paper is concerned with the free vibration of skew sandwich plates composed of an orthotropic core and laminated facings. The *p*-Ritz method has been adopted for the analysis. The Ritz functions are formed from the product of mathematically complete polynomials and boundary equations raised to appropriate integer powers depending on the boundary conditions. The boundary equations ensure the satisfaction of the geometric boundary conditions *a priori* and facilitate the handling of any type of boundary conditions. For generality, better accuracy and ease in imposition of geometric boundary condition for the oblique edges, the Ritz formulation was non-dimensionalized and cast in the skew co-ordinates system. Since no vibration solutions are available for such skew sandwich plates, the validity, convergence and accuracy of the Ritz formulation were established by comparing with other researchers' vibration frequencies for various subset plate problems involving rectangular sandwich plates and skew laminated plates. The paper features extensive generic vibration frequencies of these skew sandwich plates for various aspect ratios and boundary conditions, lamination designs of facings, material properties of core and facings.

1. INTRODUCTION

Sandwich plates have wide applications in modern engineering applications, especially in the aerospace industry. This is because they have the combination features of lightweight, high stiffness, high structural efficiency and durability.

In this paper, we consider the class of sandwich plates with laminated facings. The flexural and vibration of such sandwich plates have been studied by Monforton and Ibrahim [1, 2], Ibrahim *et al.* [3] and Kanematu and Hirano [4]. So far, investigations on such plates have been confined to the rectangular planform. The present vibration study extends these earlier works to skew sandwich plates, a planform that include the rectangular shape at the limiting value of the skew angle. For the vibration analysis, the *p*-Ritz method [5] has been adopted. The *p*-Ritz functions are formed by the product of mathematically, complete polynomials and boundary equations (that define the plate edges) raised to appropriate integer powers depending on the edge constraints. In addition to ensuring the

0022-460X/00/320317 + 24 $35.00/0

satisfaction of the geometric boundary conditions (that is crucial for convergence of the upper-bound Ritz results to the correct results), the boundary equations enable the Ritz method to be automated for skew plates with any combination of boundary conditions via the adjustment of the integer powers. For generality and better accuracy, the Ritz formulation is cast in a non-dimensional form and in the skew co-ordinates system. The skew co-ordinates system allows easy implementation of the geometric boundary conditions along the oblique edges which would otherwise be cumbersome if the rectangular Cartesian co-ordinates system was used [6].

Since there are no vibration solutions in the open literature for these skew sandwich plates with laminated facings, the Ritz results will be verified by solutions of subset plate problems that include the rectangular sandwich plates and skew laminated plates. The finite element software ABAQUS [7] is also employed to check some sample vibration solutions of the skew sandwich plates.

After establishing the correctness of the Ritz formulation and software, we generate extensive and generic vibration frequencies of such skew plates for various design parameters such as aspect ratios, boundary conditions, lamination designs of facings, material properties of core and facings. The effects of these design parameters on the natural frequencies of skew sandwich plates are also investigated and discussed. It is worth noting that the *p*-Ritz method presented herein for vibration analysis of skew sandwich plates with laminated facings can also be used for the analysis of (a) skew isotropic plates, (b) skew orthotropic plates, (c) skew laminated plates and (d) other kinds of skew sandwich plates. The vast amount of vibration results given herein should be helpful to engineers and should be useful as reference solutions for researchers.

2. *p*-RITZ METHOD FOR VIBRATION ANALYSIS

2.1. ENERGY FUNCTIONALS

Consider a skew sandwich plate of length a, oblique width b and skew angle β as shown in Figure 1. The orthotropic core (of shear moduli G_x^c, G_y^c) of the plate is sandwiched symmetrically on each surface by N layers of laminated facings. The thickness of the core is denoted by t_c, the thickness of each of the facing by t_f and the total thickness by $h = t_c + 2t_f$. Assuming the deformation of the plate's cross-section to be as shown in Figure 2, the displacement fields of the plate in the rectangular co-ordinates system can be written as

$$u_{f_1} = -z\phi_x + \frac{t_c}{2}(\phi_x - \psi_x), \quad u_{f_2} = -z\phi_x - \frac{t_c}{2}(\phi_x - \psi_x), \tag{1a, b}$$

$$v_{f_1} = -z\phi_y + \frac{t_c}{2}(\phi_y - \psi_y), \quad v_{f_2} = -z\phi_y - \frac{t_c}{2}(\phi_y - \psi_y), \tag{1c, d}$$

$$u_c = -z\psi_x, \quad v_c = -z\psi_y, \quad w_f = w_c = w_0, \tag{1e–g}$$

where u_{f_1}, v_{f_1} and u_{f_2}, v_{f_2} are the displacements in the upper and lower facings, respectively, ψ_x and ϕ_x the rotations of the core and facing in the xz plane, respectively (see Figure 2), ψ_y and ϕ_y the rotations in the yz plane, w_0 the transverse displacement at mid-plane

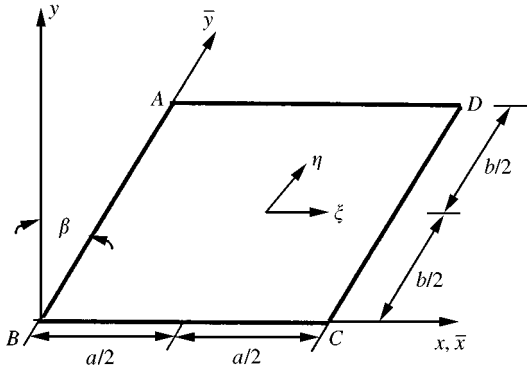

Figure 1. Co-ordinates system and dimensions of skew sandwich plate.

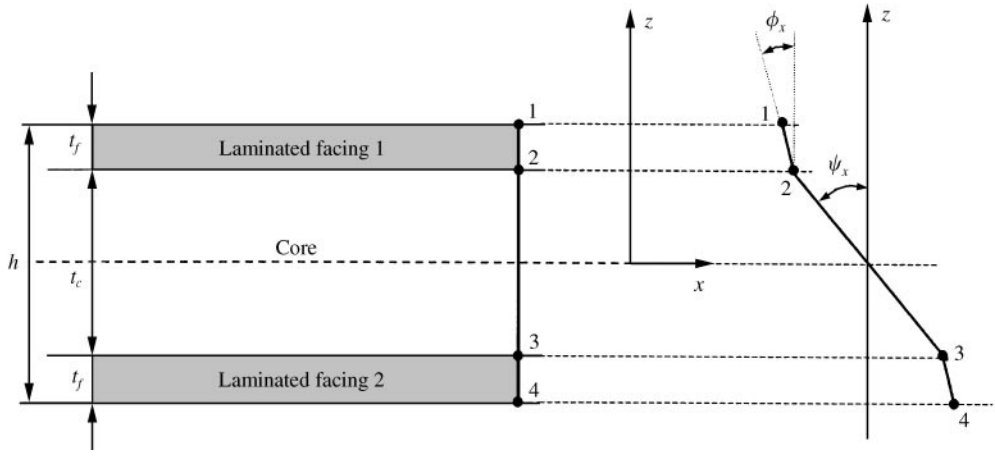

Figure 2. Deformation of cross-section of sandwich plate.

$z = 0$, and the subscripts f and c denote quantities belonging to the facings and core respectively.

When dealing with skew plates, it is expedient to use skew co-ordinates $(\bar{x}, \bar{y})$ instead of the rectangular co-ordinates (x, y) because the geometric boundary conditions of the oblique edges can be easily implemented in the p-Ritz method. From simple geometry, the relationships between these two co-ordinates systems are given by

$$\bar{x} = x - y \tan \beta, \quad \bar{y} = y \sec \beta \tag{2}$$

in which β is the skew angle as shown in Figure 1.

By adopting the skew co-ordinates system and the following non-dimensional terms,

$$\xi = \frac{2\bar{x}}{a} - 1, \quad \eta = \frac{2\bar{y}}{b} - 1 \tag{3}$$

the strain energy functionals for the facings U_f and the core U_c of the sandwich plate can be expressed as

$$U_f = \frac{ab\cos\beta}{4}\int_{-1}^{1}\int_{-1}^{1}\Big[\{\kappa\}\begin{bmatrix} D_{11} & D_{12} & D_{16} \\ & D_{22} & D_{26} \\ sym & & D_{66}\end{bmatrix}\{\kappa\}^{\mathrm{T}} + \frac{t_c^2}{4}\{\gamma\}\begin{bmatrix} A_{11} & A_{12} & A_{16} \\ & A_{22} & A_{26} \\ sym & & A_{66}\end{bmatrix}\{\gamma\}^{\mathrm{T}}$$

$$+ t_c\{\gamma\}\begin{bmatrix} \bar{B}_{11} & \bar{B}_{12} & \bar{B}_{16} \\ & \bar{B}_{22} & \bar{B}_{26} \\ sym & & \bar{B}_{66}\end{bmatrix}\{\kappa\}^{\mathrm{T}} + K_s\{\varphi\}\begin{bmatrix} A_{44} & A_{45} \\ sym & A_{55}\end{bmatrix}\{\varphi\}^{\mathrm{T}}\Big]\,\mathrm{d}\xi\,\mathrm{d}\eta, \tag{4a}$$

$$U_c = \frac{ab\cos\beta t_c}{8}\int_{-1}^{1}\int_{-1}^{1}\left(\{\gamma^c\}\begin{bmatrix} K_sG_x^c & 0 \\ sym & K_sG_y^c\end{bmatrix}\{\gamma^c\}^{\mathrm{T}} + \{\kappa^c\}\begin{bmatrix} D_c & v_cD_c & 0 \\ & D_c & 0 \\ sym. & & \dfrac{1-v_c}{2}D_c\end{bmatrix}\{\kappa^c\}^{\mathrm{T}}\right)\mathrm{d}\xi\,\mathrm{d}\eta, \tag{4b}$$

where the strain vectors are given by

$$\{\kappa\}^{\mathrm{T}} = \left\{\begin{array}{c} -\dfrac{2\cos\beta}{a}\dfrac{\partial\phi_{\bar{x}}}{\partial\xi} \\ -\dfrac{2\sin\beta\tan\beta}{a}\dfrac{\partial\phi_{\bar{x}}}{\partial\xi} + \dfrac{2\tan\beta}{b}\dfrac{\partial\phi_{\bar{x}}}{\partial\eta} + \dfrac{2\tan\beta}{a}\dfrac{\partial\phi_{\bar{y}}}{\partial\xi} - \dfrac{2\sec\beta}{b}\dfrac{\partial\phi_{\bar{y}}}{\partial\eta} \\ \dfrac{4\sin\beta}{a}\dfrac{\partial\phi_{\bar{x}}}{\partial\xi} - \dfrac{2}{b}\dfrac{\partial\phi_{\bar{x}}}{\partial\eta} - \dfrac{2}{a}\dfrac{\partial\phi_{\bar{y}}}{\partial\xi}\end{array}\right\}, \tag{5a}$$

$$\{\gamma\}^{\mathrm{T}} = \left\{\begin{array}{c} \dfrac{2\cos\beta}{a}\dfrac{\partial\Phi_{\bar{x}}}{\partial\xi} \\ \dfrac{2\sin\beta\tan\beta}{a}\dfrac{\partial\Phi_{\bar{x}}}{\partial\xi} - \dfrac{2\tan\beta}{b}\dfrac{\partial\Phi_{\bar{x}}}{\partial\eta} - \dfrac{2\tan\beta}{a}\dfrac{\partial\Phi_{\bar{y}}}{\partial\xi} + \dfrac{2\sec\beta}{b}\dfrac{\partial\Phi_{\bar{y}}}{\partial\eta} \\ -\dfrac{4\sin\beta}{a}\dfrac{\partial\Phi_{\bar{x}}}{\partial\xi} + \dfrac{2}{b}\dfrac{\partial\Phi_{\bar{x}}}{\partial\eta} + \dfrac{2}{a}\dfrac{\partial\Phi_{\bar{y}}}{\partial\xi}\end{array}\right\}, \tag{5b}$$

$$\{\varphi\}^{\mathrm{T}} = \left\{\begin{array}{c} \phi_{\bar{x}}\sin\beta - \phi_{\bar{y}} - \dfrac{2\tan\beta}{a}\dfrac{\partial w_0}{\partial\xi} + \dfrac{2\sec\beta}{b}\dfrac{\partial w_0}{\partial\eta} \\ -\phi_{\bar{x}}\cos\beta + \dfrac{2}{a}\dfrac{\partial w_0}{\partial\xi}\end{array}\right\}, \tag{5c}$$

$$\{\gamma^c\}^{\mathrm{T}} = \left\{\begin{array}{c} -\psi_{\bar{x}}\cos\beta + \dfrac{2}{a}\dfrac{\partial w_0}{\partial\xi} \\ \psi_x\sin\beta - \psi_y - \dfrac{2\tan\beta}{a}\dfrac{\partial w_0}{\partial\xi} + \dfrac{2\sec\beta}{b}\dfrac{\partial w_0}{\partial\eta}\end{array}\right\} \tag{5d}$$

in which $\Phi = \phi - \psi$, K_s is the shear correction factor and $A_{ij} = A_{ij}^1 + A_{ij}^2$, $D_{ij} = D_{ij}^1 + D_{ij}^2$, $\bar{B}_{ij} = B_{ij}^1 - B_{ij}^2$, where A_{ij}^n, B_{ij}^n, $D_{ij}^n (n = 1, 2)$ are the extensional, coupling and bending stiffnesses of the two laminated facings respectively.

The kinetic energy functionals for the facings T_f and for the core T_c are given by

$$T_f = \frac{ab\rho_f \cos\beta}{4}\omega^2 \int_{-1}^{1}\int_{-1}^{1}\int_{t_c/2}^{t_c/2+t_f} [u_f^2 + v_f^2 + w_f^2]\,\mathrm{d}z\,\mathrm{d}\xi\,\mathrm{d}\eta, \tag{7a}$$

$$T_c = \frac{ab\rho_c \cos\beta}{8}\omega^2 \int_{-1}^{1}\int_{-1}^{1}\int_{-t_c/2}^{t_c/2} [u_c^2 + v_c^2 + w_0^2]\,\mathrm{d}z\,\mathrm{d}\xi\,\mathrm{d}\eta, \tag{7b}$$

where ω is the angular frequency of the plate, and ρ_f, ρ_c are the mass densities of the facings and the core respectively.

The Lagrangian of the sandwich plate is thus given by

$$\Pi = T_f + T_c - U_f - U_c. \tag{8}$$

2.2. GOVERNING EIGENVALUE EQUATION

To solve the plate problem at hand, the p-Ritz method is used where the Ritz functions (in skew co-ordinates) for approximating the displacement fields are taken as

$$\bar{w}_o(\bar{\xi}, \bar{\eta}) = \frac{w_o(\bar{\xi}, \bar{\eta})}{(t_c + 2t_f)} = \sum_{q=0}^{p}\sum_{i=0}^{q} c_k \chi_k^w(\bar{\xi}, \bar{\eta}), \tag{9a}$$

$$\phi_{\bar{x}}(\bar{\xi}, \bar{\eta}) = \sum_{q=0}^{p}\sum_{i=0}^{q} \mathrm{d}_k \chi_k^f(\bar{\xi}, \bar{\eta}), \qquad \phi_{\bar{y}}(\bar{\xi}, \bar{\eta}) = \sum_{q=0}^{p}\sum_{i=0}^{q} e_k \chi_k^g(\bar{\xi}, \bar{\eta}), \tag{9b,c}$$

$$\psi_{\bar{x}}(\bar{\xi}, \bar{\eta}) = \sum_{q=0}^{p}\sum_{i=0}^{q} f_k \chi_k^d(\bar{\xi}, \bar{\eta}), \qquad \psi_{\bar{y}}(\bar{\xi}, \bar{\eta}) = \sum_{q=0}^{p}\sum_{i=0}^{q} g_k \chi_k^e(\bar{\xi}, \bar{\eta}), \tag{9d,e}$$

where p is the degree set of the complete polynomial space, $(c, d, \ldots, g)$ are the unknown coefficients, and the subscript k is given by

$$k = \frac{(q+1)(q+2)}{2} - i. \tag{10}$$

The adopted functions χ_k are

$$[\chi_k^w(\bar{\xi}, \bar{\eta}), \chi_k^d(\bar{\xi}, \bar{\eta}), \chi_k^e(\bar{\xi}, \bar{\eta}), \chi_k^f(\bar{\xi}, \bar{\eta}), \chi_k^g(\bar{\xi}, \bar{\eta})]$$
$$= \bar{\xi}^i \bar{\eta}^{q-i} [\chi_1^w(\bar{\xi}, \bar{\eta}), \chi_1^d(\bar{\xi}, \bar{\eta}), \chi_1^e(\bar{\xi}, \bar{\eta}), \chi_1^f(\bar{\xi}, \bar{\eta}), \chi_1^g(\bar{\xi}, \bar{\eta})], \tag{11}$$

where the basic functions χ_1 are formed by the boundary equations raised to appropriate powers as shown below:

$$\langle \chi_1^w(\bar{\xi}, \bar{\eta}), \chi_1^d(\bar{\xi}, \bar{\eta}), \ldots, \chi_1^g(\bar{\xi}, \bar{\eta})\rangle = \left\langle \prod_{j=1}^{4} [\zeta_j(\bar{\xi}, \bar{\eta})]^{\gamma_j^w}, \prod_{j=1}^{4} [\zeta_j(\bar{\xi}, \bar{\eta})]^{\gamma_j^d}, \ldots, \prod_{j=1}^{4} [\zeta_j(\bar{\xi}, \bar{\eta})]^{\gamma_j^g} \right\rangle \tag{12}$$

and $\zeta_1 = (\xi + 1)$, $\zeta_2 = (\eta + 1)$, $\zeta_3 = (\xi - 1)$, and $\zeta_4 = (\eta - 1)$.

The powers γ_j in equation (12) depend on the supporting edge condition and are given as follows:

$$\gamma_j^w = \begin{cases} 0 & \text{free (F),} \\ 1 & \text{simply supported (S) or clamped (C),} \end{cases} \tag{13a}$$

$$\gamma_j^d = \begin{cases} 0 & \text{free (F) or simply supported (S) in } y \text{ direction,} \\ 1 & \text{simply supported (S) in } x \text{ direction or clamped (C),} \end{cases} \tag{13b}$$

$$\gamma_j^e = \begin{cases} 0 & \text{free (F) or simply supported (S) in } x \text{ direction,} \\ 1 & \text{simply supported (S) in } y \text{ direction or clamped (C),} \end{cases} \tag{13c}$$

$$\gamma_j^f = \begin{cases} 0 & \text{free (F) or simply supported (S) in } y \text{ direction,} \\ 1 & \text{simply supported (S) in } x \text{ direction or clamped (C),} \end{cases} \tag{13d}$$

$$\gamma_j^g = \begin{cases} 0 & \text{free (F) or simply supported (S) in } x \text{ direction,} \\ 1 & \text{simply supported (S) in } y \text{ direction or clamped (C).} \end{cases} \tag{13e}$$

Applying the Ritz method,

$$\left\langle \frac{\partial \Pi}{\partial c_k}, \frac{\partial \Pi}{\partial d_k}, \frac{\partial \Pi}{\partial e_k}, \frac{\partial \Pi}{\partial f_k}, \frac{\partial \Pi}{\partial g_k} \right\rangle = \langle 0, 0, 0, 0, 0 \rangle, \tag{14}$$

where $k = 1, 2, \ldots, (p+1)(p+2)/2$. The substitution of equations (4), (7) and (8) into equation (14) yields the following governing eigenvalue equation:

$$([K] - \Omega^2[M])\{\Theta\} = \{0\} \tag{15}$$

in which $\Omega = \omega a \sqrt{\rho_c / E_{11}} \times 10^2$ is the frequency parameter, $[K]$, $[M]$ are the stiffness and mass matrices, respectively, and their elements are given in Appendix A. The eigenvalue problem may be solved using any standard eigenvalue solver for the natural frequencies. We have adopted the RSG subroutine of EISPACK [8] as the eigenvalue solver.

3. NUMERICAL RESULTS

3.1. CONVERGENCE AND COMPARISON STUDIES

3.1.1. *Rhombic laminated plates*

Consider a 45° rhombic, laminated plate composed of five symmetric cross-ply layers with all its four edges clamped. This plate example was treated earlier by Wang [9], who also used the Ritz method but employed B-splines as the Ritz functions. The total thickness of the equal-thickness laminates is taken as $h/a = 0{\cdot}1$. The material properties for each lamina are identical and are taken as $E_{11}/E_{22} = 40{\cdot}0$, $G_{12}/E_{22} = 0{\cdot}6$, $G_{23}/E_{22} = 0{\cdot}5$, $\nu_{23} = 0{\cdot}25$. This subset plate problem can be readily handled by the general Ritz formulation through setting the core thickness of the sandwich plate to be negligible (say $t_c/h = 10^{-10}$).

TABLE 1

Frequency parameters $\bar{\Omega} = (\omega b^2/\pi^2 h)\sqrt{\rho/E_{22}}$ *of CCCC* 45° *rhombic cross-ply* (90°/0°/90°/0°/90°) *laminates*

Polynomial degree p	Mode sequence number							
	1	2	3	4	5	6	7	8
4	3·4940	4·9180	6·3925	6·5433	8·4678	9·7206	9·9977	11·9561
6	3·4779	4·7583	6·0181	6·4152	7·7897	8·1136	9·3619	9·6883
8	3·4752	4·7407	5·9603	6·3833	7·2794	8·0206	8·6187	9·5193
10	3·4744	4·7395	5·9551	6·3767	7·1972	7·9992	8·4414	9·4387
12	3·4741	4·7394	5·9547	6·3752	7·1902	7·9960	8·4184	9·3952
14	3·4738	4·7393	5·9546	6·3747	7·1898	7·9957	8·4167	9·3880
Wang [9]	3·4738	4·7393	5·9554	6·3750	7·1961	8·0031	8·4468	9·4414

Table 1 shows a typical convergence study of the first eight frequency parameters $\bar{\Omega} = (\omega l^2/\pi^2 h)\sqrt{\rho/E_{22}}$ with respect to the degree of polynomial functions. The results display a monotonic and rapid convergence. It can be seen that a polynomial degree of 12 will suffice in yielding accurate vibration results for all purposes. Further, the converged results check out with those obtained by Wang [9].

3.1.2. *Skew sandwich plates*

Next, convergence studies are conducted for simply supported skew plates with two symmetric cross-ply layers of facing, i.e., (0°/90°/core/90°/0°), an aspect ratio of $a/b = 2$, skew angles $\beta = 0$ and 30°, and thickness-to-width ratio $h/b = 0{\cdot}05$, the core thickness to total thickness ratio t_c/h is 0·8. In order to compare with Ibrahim *et al.* [3] results, the material properties for the core and facings are taken to be

$$\frac{E_{11}}{E_{22}} = 40{\cdot}0, \quad \frac{G_{12}}{E_{22}} = 1{\cdot}0, \quad \nu_{12} = 0{\cdot}25, \quad \nu_{23} = 0.3, \quad \frac{G_x^c}{E_c} = \frac{1{\cdot}173}{6{\cdot}279}, \quad \frac{G_y^c}{E_c} = \frac{2{\cdot}415}{6{\cdot}279}, \quad \frac{\rho_f}{\rho_c} = 0.6818. \tag{16}$$

The first four frequency parameters $\Omega = \omega a\sqrt{\rho_c/E_{11}} \times 10^2$ obtained by the *p*-Ritz method are presented in Table 2 for different degrees of polynomial space *p*. It can be seen that a relatively lower degree of polynomial ($p = 8$) will suffice for converged results in the case of the rectangular plate ($\beta = 0°$), as compared to a higher polynomial degree ($p = 12$) required for the skew plate with $\beta = 30°$. The tabulated results are found to compare well with the Fourier series solutions obtained by Ibrahim *et al.* [3]. The results are also in good agreement with the finite element results given by the software ABAQUS [7] (where we use the composite thick shell element S8R and a uniform mesh size of 16×8 mesh having a total number of degrees of freedom equal to 2598). It is worth noting that the *p*-Ritz method (using a polynomial degree $p = 12$ for all the Ritz functions that amounts to a total of 455 degrees of freedom) gave more accurate results than the finite element method. In addition to the use of a lesser number of degrees of freedom, the *p*-Ritz method has a faster rate of convergence with respect to increasing number of degrees of freedom when compared to ABAQUS.

TABLE 2

Convergence and comparison studies of skew sandwich SSSS plates

β	P		Mode sequence number 1	2	3	4
0°	Present study	4	12·424	16·725	26·832	34·180
		6	12·420	16·696	23·880	32·164
		8	12·420	16·696	23·747	31·767
		10	12·420	16·696	23·745	31·755
	Ibrahim *et al.* [3]		12·418	16·705	23·773	—
	ABAQUS (8×16 mesh)		12·456	16·742	23·773	31·742
30°	Present study	4	15·965	20·418	32·713	41·486
		8	15·782	20·029	26·886	34·467
		10	15·767	20·007	26·823	34·346
		12	15·758	19·992	26·805	34·331
	ABAQUS (8×16 mesh)		15·773	20·084	26·915	34·388

Based on the foregoing convergence and comparison studies, it can be concluded that the *p*-Ritz method gives very accurate vibration results for the considered skew plates. Below, we use the method to generate new sets of vibration frequencies of skew sandwich plates with laminated facings and we shall also investigate the effects of various design parameters on the frequencies.

3.2. EFFECT OF PLATE THICKNESS AND MATERIAL PROPERTIES

To investigate the effects of core thickness and the total plate thickness on the frequency parameter Ω, the simply supported rhombic sandwich plates with orthotropic core and cross-ply layers for the facings (0°/90°/core/90°/0°) are adopted. The plate skew angle $\beta = 30°$ and the total thickness to length ratio h/a is taken to be 0·001, 0·005, 0·01, 0·05 and 0·1. Two different material properties for the core and facings are selected:

$$\textit{Type 1: } \frac{E_{11}}{E_{22}} = 40{\cdot}0, \quad \frac{G_{12}}{E_{22}} = 1{\cdot}0, \quad \nu_{12} = 0{\cdot}25, \quad \nu_{23} = 0{\cdot}3, \quad \frac{G_x^c}{E_c} = \frac{1{\cdot}173}{6{\cdot}279}, \quad \frac{G_y^c}{E_c} = \frac{2{\cdot}415}{6{\cdot}279}, \quad \frac{\rho_f}{\rho_c} = 0{\cdot}6818, \tag{17a}$$

$$\textit{Type 2: } \frac{E_{11}}{E_{22}} = \frac{130{\cdot}8}{10{\cdot}6}, \quad \frac{G_{12}}{E_{22}} = \frac{6}{10{\cdot}6}, \quad \nu_{12} = 0{\cdot}28, \quad \nu_{23} = 0{\cdot}34, \quad \frac{G_x^c}{E_c} = \frac{5{\cdot}206}{30{\cdot}13}, \quad \frac{G_y^c}{E_c} = \frac{1{\cdot}772}{30{\cdot}13}, \quad \frac{\rho_f}{\rho_c} = 15.659. \tag{17b}$$

Although both sandwich plate designs have facings that are relatively stiffer than the core, the Type 1 sandwich plate has a much heavier core than Type 2 sandwich plate. Note that Type 1 has a glass fiber honeycomb core (which is the same as that defined in equation (16))

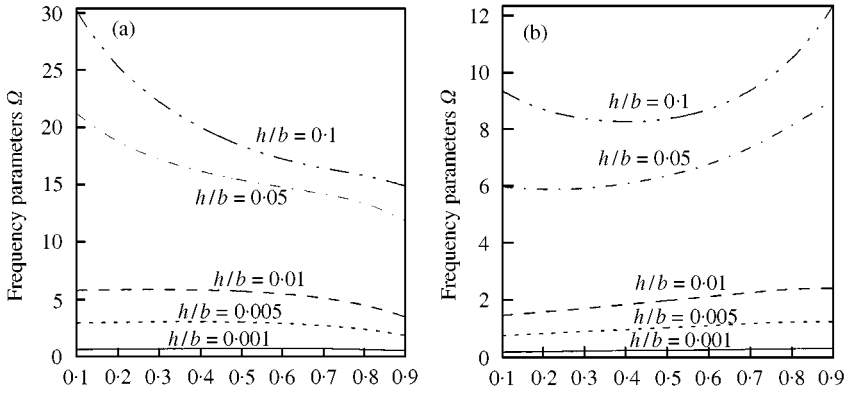

Figure 3. Effect of core thickness on fundamental frequency Ω_1 of rhombic sandwich SSSS plates. Core thickness to total plate thickness ratio t_0/h: (a) heavy core; (b) light core.

while Type 2 has an aluminum honeycomb core. By considering these two material types, one may examine the vibration behavior of sandwich plates with a heavy core (Type 1) against their counterparts with a lighter core (Type 2).

Figures 3(a) and 3(b) show both the effects of varying core thickness (t_c/h) and total plate thickness (h/b) on the fundamental frequency of vibration. The vibration behavior is rather different for the two kinds of sandwich plates. It can be observed from Figure 3(a) that the plate with a heavier core (Type 1 material) has fundamental frequency parameters decreasing (for all plate thickness to length ratios h/b) with increasing core thickness. This trend may be explained by the fact that as the core thickness increases, the sandwich plate becomes heavier and more flexible; thus lowering its stiffness against vibration. On the other hand, with a lighter core (Type 2 material), the plate's fundamental frequency parameter, for thick plates ($h/b = 0{\cdot}05$ and $0{\cdot}1$), will first decrease and later increase as the core thickness ratio (t_c/h) increases as shown in Figure 3(b). This is due to the fact that for thick plates, as the core thickness increases, the plate becomes less stiff leading to a lowering of the frequency value but at the same time the plate is also getting lighter which causes the frequency value to increase. Thus, there is a trade-off between plate rigidities and mass effects on the natural frequencies for this case. However, for relatively thin plates ($h/b < 0{\cdot}01$), the frequency parameter increases monotonically with increasing core thickness ratio because the effect of decreasing flexural rigidity has been overshadowed by the effect of decreasing mass density.

3.3. EFFECT OF BOUNDARY CONDITIONS

To study the effect of boundary conditions on the vibration frequencies, six combinations of free, simply supported and clamped edge boundary conditions, designated as SSSS, SCSC, CCCC, FSFS, FCFC, and CFFF, are considered as shown in Figure 4. The letters F, S and C denote free, simply supported and clamped edges respectively. The skew sandwich plates analyzed here have an aspect ratio a/b of 1 and thickness-to-width ratios $h/b = 0{\cdot}1$ and $0{\cdot}001$. The orthotropic core of the plate is sandwiched by two symmetric cross-ply facings ($0^\circ/90^\circ$/core/$90^\circ/0^\circ$). Their material properties are defined in equation (16) and the core thickness to total thickness ratio $t_c/h = 0{\cdot}8$. The influences of boundary conditions on the fundamental frequency are shown in Figures 5(a) and 5(b). It can be seen that the

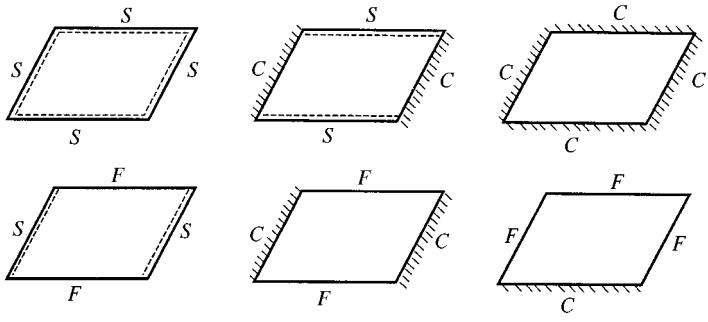

Figure 4. Skew plates with various boundary conditions.

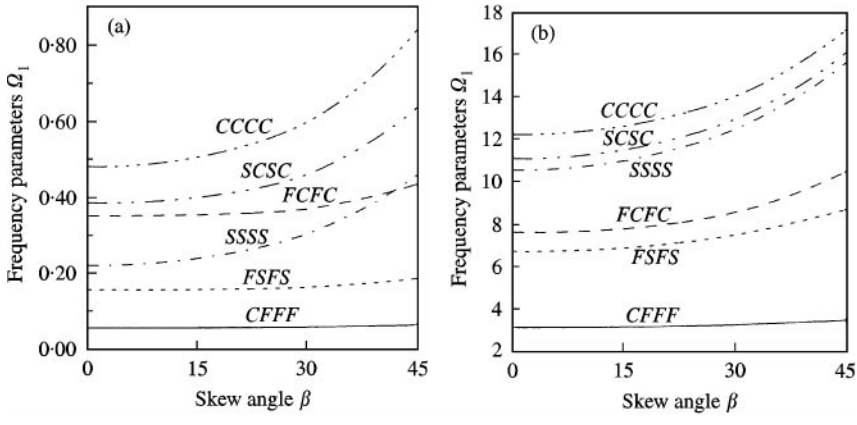

Figure 5. Effect of boundary conditions on fundamental frequency parameter Ω_1 of rhombic sandwich plates. Skew angle β: (a) $h/b = 0{\cdot}001$; (b) $h/b = 0{\cdot}1$.

fundamental frequency increases with greater geometric constraint been imposed at the four edges in the following sequence: CFFF, FSFS, FCFC (SSSS and FCFC may swap places depending on the plate thickness), SCSC and CCCC. Among these edge conditions, the 45° CCCC plate has the highest fundamental frequency which is about 5–12 times higher than its CFFF counterpart depending on the plate thickness. It can also be observed that as the skew angle decreases, the frequency parameter decreases for all plates, especially for the case of CCCC plates. For thick plates ($h/b = 0{\cdot}1$), the fundamental frequency of SSSS boundary condition is higher than that of FCFC condition. On the other hand, when the plate is very thin ($h/b = 0{\cdot}001$), the fundamental frequency of FCFC plate is higher than that of SSSS plate except when the skew angle is greater than 45°. It appears that for thick plates, the simply supported constraint is more effective than having two clamped oblique sides while free on the other two parallel sides.

3.4. EFFECT OF SKEW ANGLE

To investigate the effect of skew angle on the frequencies, we consider simply supported, skew (rhombic) sandwich plates with one-layer facings. The core may be made of an

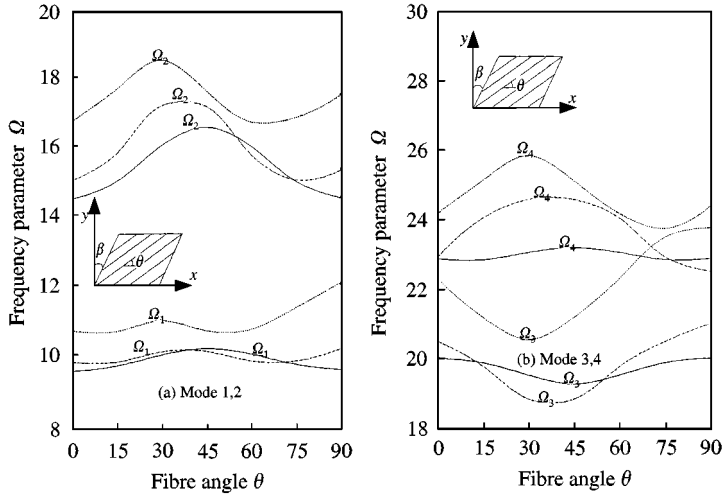

Figure 6. Effect of skew angle on frequency parameter Ω of skew sandwich SSSS plates with isotropic core [$a/b = 1$, $h/b = 0{\cdot}1$, $t_c/t_f = 8$, (θ/core/θ)]. ····· $\beta = 30°$; ----- $\beta = 15°$; —— $\beta = 0°$.

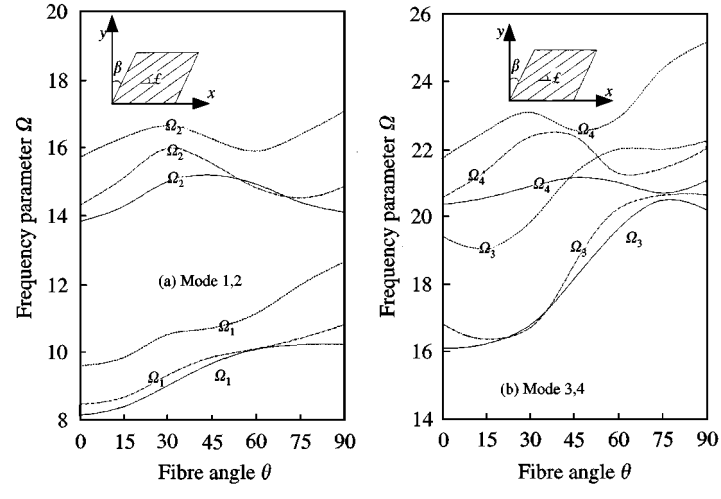

Figure 7. Effect of skew angle on frequency parameter Ω of skew sandwich SSSS plates with orthotropic core [$a/b = 1$, $h/b = 0{\cdot}1$, $t_c/t_f = 8$, (θ/core/θ)]. ····· $\beta = 30°$; ----- $\beta = 15°$; —— $\beta = 0°$.

isotropic material or an orthotropic material. The first four frequencies of such skew sandwich plates are presented in Figures 6 and 7 for plates with isotropic core and orthotropic core respectively.

Since the results in Figure 6 are based on sandwich plates with an isotropic core, the frequency curves for square sandwich plates ($\beta = 0^{\circ}$) are symmetric with respect to fibre angle $\theta = 45°$. Interestingly, the frequency curves for skew sandwich plates with skew angles $\beta = 15°$ and $30°$ become symmetric with respect to $\theta = 37{\cdot}5°$ and $30°$ respectively. It means that for such rhombic sandwich plates with isotropic core, the frequencies for both cases are the same when the orientation of the fibre is parallel to either skew coordinates axis.

It can be observed in Figure 7 that the frequency parameter generally increases with increasing values of skew angle for a given facing fibre orientation, except for some cases of fibre orientations. For example, the frequency for a sandwich plate with a skew angle $\beta = 15^\circ$ is lower than for a rectangular sandwich plate when the fibre angle θ is in the range of 55°–70°. For a fixed skew angle, the fundamental frequency parameter Ω_1 is found to increase with increasing facing fibre angles θ. This is because the orthotropic core considered here is stiffer in the y direction than in the x direction. The maximum value of frequency for the second mode is apparently in the neighborhood of $\theta = 30^\circ$, whilst for the third mode the corresponding value for θ is between 60° and 75°. For the fourth mode, the maximum frequency occurs when θ is between 30° and 45°. Based on the foregoing observations, it can be concluded that the vibration frequencies are significantly affected by the skew angle.

3.5. EFFECT OF FIBRE ORIENTATION

Figures 8–11 show the effect of fibre orientation on the frequency parameter Ω for simply supported rhombic sandwich plates. The plates considered have an aspect ratio $a/b = 1{\cdot}0$, total thickness to length ratio $h/b = 0{\cdot}1$ and thickness of core to total thickness ratio $t_c/h = 0{\cdot}8$. In Figures 9 and 10, the facing comprises of four symmetric angle-ply layers, i.e., $(\theta_1/\theta_2/\theta_1/\theta_2/\text{core}/\theta_2/\theta_1/\theta_2/\theta_1)$ with $\theta_2 - \theta_1 = 30°$. In Figures 10 and 11, the facing considered have two angle-ply layers, i.e., $(\theta/-\theta/\text{core}/-\theta/\theta)$.

The core considered in Figure 8 is assumed to be isotropic. It can be seen that for the case of $\beta = 0^\circ$, the natural frequencies are the same when the fibre angle θ_1 of the first facing layer takes the value of 0 and 90°. For the fundamental frequency Ω_1, the fibre orientation has negligible effect for square plates. However, the fibre orientation has a more pronounced effect on other frequencies and skew plates.

The core of sandwich plate in Figure 9 is assumed to be an orthotropic core. It can be seen that the fibre orientation has a greater effect on the fundamental frequency Ω_1 and on the third frequency Ω_3 when compared to its effect on the second and fourth frequencies. When the fibre angle of the first facing layer θ_1 is less than 60°, the frequency curves for

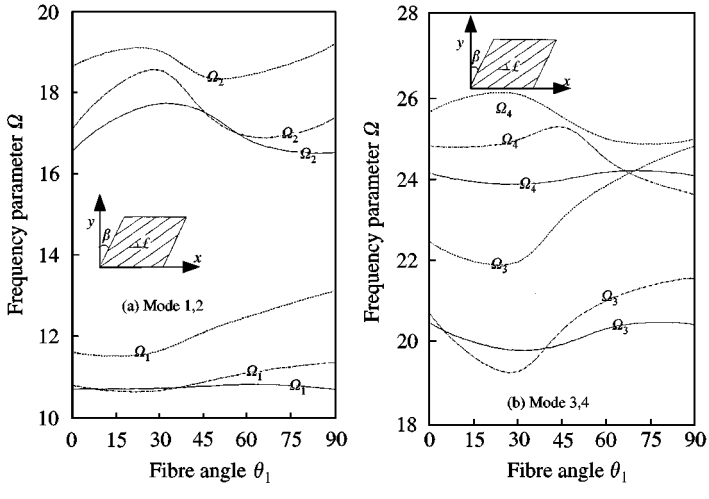

Figure 8. Effect of fibre orientation on frequency parameter Ω of skew sandwich SSSS plates with isotropic core $[a/b = 1,\ h/b = 0{\cdot}1,\ t_c/t_f = 8,\ (\theta1/\theta2/\theta1/\theta2/\text{core}/\theta2/\theta1/\theta2/\theta1),\ \theta2 - \theta1 = 30^\circ]$. ····· $\beta = 30^\circ$; ----- $\beta = 15^\circ$; —— $\beta = 0^\circ$.

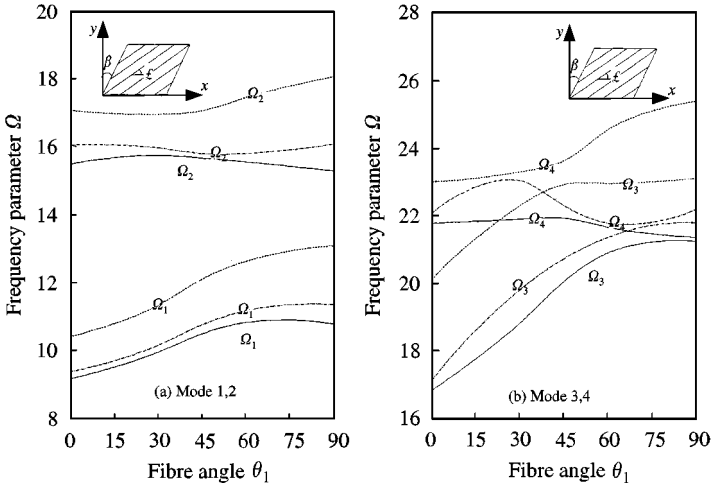

Figure 9. Effect of fibre orientation on frequency parameter Ω of skew sandwich SSSS plates with orthotropic core [$a/b = 1$, $h/b = 0{\cdot}1$, $t_c/t_f = 8$, ($\theta1/\theta2/\theta1/\theta2$/core/$\theta2/\theta1/\theta2/\theta1$), $\theta2 - \theta1 = 30°$]. ····· $\beta = 30°$; - - - - - $\beta = 15°$; —— $\beta = 0°$.

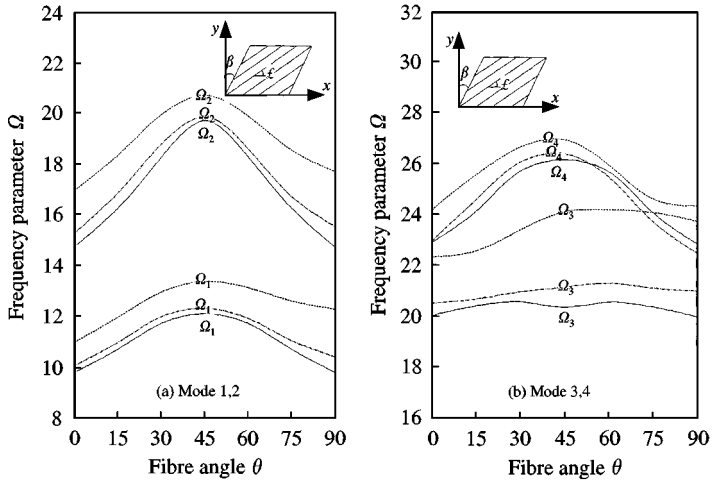

Figure 10. Effect of fibre orientation on frequency parameter Ω of skew sandwich SSSS plates with isotropic core [$a/b = 1$, $h/b = 0{\cdot}1$, $t_c/t_f = 8$, ($\theta/-\theta$/core/$-\theta/\theta$)]. ····· $\beta = 30°$; - - - - - $\beta = 15°$; —— $\beta = 0°$.

Ω_1 and Ω_3 vary significantly. When θ_1 is greater than 60^0, the curves are rather flat, i.e., the frequencies do not vary much with respect to the fibre angle.

In Figure 10, we present results for simply supported skew sandwich plates composed of an isotropic core and two symmetric angle-ply layers of facing. It can be observed that the frequency curves for square plates are symmetric with respect to $\theta = 45°$, and the frequency has its peak value at $\theta = 45°$. The maximum values of frequency parameters Ω_1, Ω_2 and Ω_4 appear at $\theta = 45°$ for skew plates. However, the maximum values of frequency parameters Ω_3 appear to be around $\theta = 30°$ and $60°$. For skew sandwich plates ($\beta = 15$ and $30°$), the frequency curves of Ω_1, Ω_2 and Ω_4 become nearly symmetric with respect to $\theta = 45°$.

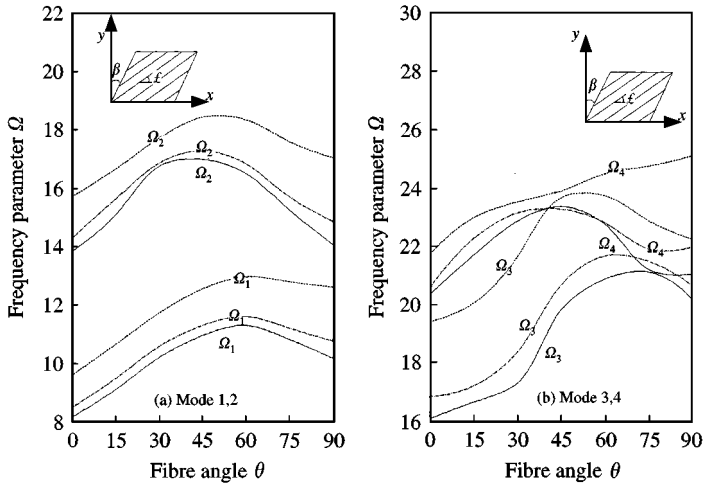

Figure 11. Effect of fibre orientation on frequency parameter Ω of skew sandwich SSSS plates with orthotropic core [$a/b = 1$, $h/b = 0{\cdot}1$, $t_c/t_f = 8$, $(\theta/-\theta/\text{core}/-\theta/\theta)$]. ····· $\beta = 30°$; - - - - - $\beta = 15°$; —— $\beta = 0°$.

Next we consider an orthotropic core. Referring to Figure 11, the frequency curves of Ω_1, Ω_2 and Ω_3 reach their peak values around $\theta = 45°-60°$. In view of the orthotropic core being stiffer in the y direction, the effect of fibre orientation is found to be more significant when $\theta < 45°$.

3.6. TABULATED RESULTS FOR SANDWICH PLATES

As there is a dearth of vibration results for skew sandwich plates with laminated facings, we present in Tables 3 and 4 the first four frequencies of skew sandwich plates composed of an orthotropic core and laminated facings with different numbers of symmetric cross-ply layers $N = 2, 4, 8$, i.e., $(0°/90°/\ldots/90°/\text{core}/90°/\ldots/90°/0°)$. The core thickness to total thickness ratio $t_c/h = 0{\cdot}8$. The material properties are defined in equation (16).

In particular, Table 3 gives results for SSSS plates with aspect ratios $a/b = 1{\cdot}0$ and $2{\cdot}0$, thickness-to-width ratios $h/b = 0{\cdot}05$, $0{\cdot}10$ and $0{\cdot}15$ (while keeping a constant oblique length b) and the skew angles $\beta = 0°$, $15°$, $30°$ and $45°$. Table 4 gives the natural frequencies of CSCS, CCCC, FSFS, FCFC and FCFF plates with an aspect ratio $a/b = 1{\cdot}0$, and thickness-to-width ratio $b/h = 0{\cdot}05$. These tabulated frequency parameters should be useful as benchmark solutions for researchers who are developing numerical techniques and software for solving skew sandwich plate vibration problems.

4. CONCLUDING REMARKS

The p-Ritz formulation, cast in a non-dimensional form and in the skew co-ordinates system, has been successfully developed and coded for the free vibration analysis of skew sandwich plates composed of an orthotropic core and laminated facings. Using a set of Ritz functions involving polynomial functions and boundary equations raised to appropriate powers that depend on the boundary conditions, the p-Ritz method is made automated for the analysis of such sandwich plates with any combination of edge conditions. Owing to the

TABLE 3

Frequency parameters Ω of skew sandwich SSSS plates

a/b	h/b	Skew angle β (deg)	Number of facing layers	Mode sequence number			
				1	2	3	4
			2	8·029	14·858	16·984	21·111
		0	4	8·068	14·693	17·401	21·321
			8	8·086	14·597	17·595	21·408
			2	8·470	15·190	18·000	21·007
		15	4	8·526	15·085	18·407	21·082
	0·05		8	8·551	15·014	18·599	21·079
			2	9·982	16·544	21·159	21·910
		30	4	10·094	16·547	21·628	21·997
			8	10·145	16·525	21·843	21·998
			2	13·232	19·563	24·655	27·496
		45	4	13·460	19·708	24·841	28·189
			8	13·562	19·749	24·884	28·490
			2	10·555	16·830	19·648	23·616
		0	4	10·660	16·859	20·233	24·079
			8	10·704	16·823	20·476	24·240
			2	11·010	17·231	20·586	23·184
		15	4	11·136	17·312	21·193	23·578
1·0	0·10		8	11·188	17·299	21·441	23·660
			2	12·521	18·655	23·600	24·005
		30	4	12·715	18·857	24·340	24·471
			8	12·796	18·896	24·580	24·627
			2	15·672	21·746	26·831	29·777
		45	4	16·017	22·149	27·497	30·936
			8	16·158	22·266	27·676	31·348
			2	11·414	17·552	20·426	24·436
		0	4	11·579	17·842	21·216	25·229
			8	11·642	17·876	21·505	25·469
			2	11·857	17·952	21·365	24·024
		15	4	12·049	18·296	22·210	24·903
	0·15		8	12·121	18·354	22·512	25·117
			2	13·331	19·373	24·413	24·872
		30	4	13·610	19·862	25·501	25·878
			8	13·715	19·978	25·863	26·125
			2	16·427	22·512	27·809	30·774
		45	4	16·914	23·281	29·137	32·564
			8	17·090	23·491	29·474	33·107
			2	12·063	16·058	22·473	29·715
		0	4	12·350	16·136	22·318	29·386
			8	12·489	16·172	22·230	29·194
			2	12·767	16·748	23·107	30·212
		15	4	13·075	16·855	22·989	29·942
	0·05		8	13·225	16·904	22·918	29·777
			2	15·196	19·127	25·325	32·145
		30	4	15·579	19·328	25·316	32·009
			8	15·763	19·421	25·296	31·906
			2	20·572	24·357	30·230	36·644
		45	4	21·120	24·750	30·435	36·730
			8	21·379	24·931	30·515	36·731

TABLE 3

Continued

a/b	h/b	Skew angle β (deg)	Number of facing layers	Mode sequence number			
				1	2	3	4
			2	16·984	21·111	26·981	33·661
		0	4	17·401	21·321	27·041	33·718
			8	17·595	21·408	27·027	33·645
			2	17·746	21·849	27·683	34·259
		15	4	18·192	22·095	27·785	34·374
2·0	0·10		8	18·399	22·198	27·791	34·329
			2	20·310	24·322	30·041	36·387
		30	4	20·852	24·683	30·276	36·656
			8	21·101	24·836	30·340	36·679
			2	25·779	29·575	35·056	41·126
		45	4	26·537	30·182	35·566	41·686
			8	26·875	30·437	35·743	41·830
			2	18·815	22·828	28·493	35·104
		0	4	19·315	23·158	28·805	35·684
			8	19·537	23·284	28·865	35·752
			2	19·556	23·555	29·194	35·709
		15	4	20·091	23·928	29·559	36·349
	0·15		8	20·327	24·071	29·639	36·445
			2	22·045	25·984	31·547	37·858
		30	4	22·700	26·499	32·077	38·679
			8	22·981	26·696	32·223	38·850
			2	27·373	31·155	36·563	42·672
		45	4	28·310	31·990	37·456	43·879
			8	28·694	32·304	37·733	44·189

TABLE 4

Frequency parameters Ω of skew sandwich plates with various boundary conditions ($a/b = 1·0$, $h/b = 0·05$)

Boundary condition	Skew angle β (deg)	Number of facing layers	Mode sequence number			
			1	2	3	4
		2	9·098	15·441	17·442	21·516
	0	4	9·150	15·450	17·861	21·840
		8	9·155	15·387	18·046	21·945
		2	9·487	15·722	18·452	21·418
	15	4	9·553	15·771	18·874	21·646
SCSC		8	9·566	15·734	19·056	21·683
		2	10·880	17·010	21·589	22·308
	30	4	10·999	17·148	22·088	22·540
		8	11·037	17·163	22·295	22·581
		2	14·002	20·106	25·181	27·925
	45	4	14·251	20·405	25·539	28·682
		8	14·346	20·494	25·632	28·983

TABLE 4

Continued

Boundary condition	Skew angle β (deg)	Number of facing layers	Mode sequence number			
			1	2	3	4
CCCC	0	2	10·930	16·498	18·650	22·483
		4	11·112	16·594	19·255	22·969
		8	11·171	16·569	19·485	23·117
	15	2	11·342	16·830	19·591	22·413
		4	11·543	16·969	20·209	22·765
		8	11·610	16·967	20·441	22·826
	30	2	12·762	18·201	22·571	23·429
		4	13·029	18·444	23·294	23·802
		8	13·122	18·490	23·557	23·874
	45	2	15·850	21·424	26·481	28·732
		4	16·274	21·869	27·031	29·773
		8	16·424	21·993	27·166	30·134
FSFS	0	2	5·376	5·902	13·477	13·849
		4	5·254	5·800	13·214	13·755
		8	5·190	5·748	13·066	13·624
	15	2	5·449	6·317	13·522	13·736
		4	5·327	6·240	13·475	13·509
		8	5·263	6·198	13·328	13·469
	30	2	5·727	7·534	14·262	14·711
		4	5·608	7·530	14·247	14·477
		8	5·544	7·514	14·205	14·339
	45	2	6·310	9·065	15·533	16·839
		4	6·209	9·089	15·470	16·744
		8	6·150	9·061	15·386	16·658
FCFC	0	2	7·004	7·266	14·135	14·362
		4	6·929	7·206	14·067	14·560
		8	6·865	7·151	13·959	14·465
	15	2	7·120	7·580	14·034	14·409
		4	7·046	7·531	14·127	14·346
		8	6·984	7·482	14·121	14·244
	30	2	7·701	8·622	14·756	15·602
		4	7·648	8·609	14·837	15·582
		8	7·599	8·577	14·832	15·507
	45	2	9·289	10·787	16·818	18·433
		4	9·313	10·849	16·933	18·539
		8	9·298	10·851	16·938	18·520
CFFF	0	2	2·224	2·869	9·577	10·376
		4	2·291	2·922	9·901	10·669
		8	2·322	2·947	10·043	10·796
	15	2	2·014	3·247	9·122	10·500
		4	2·064	3·314	9·367	10·706
		8	2·087	3·345	9·465	10·775
	30	2	1·816	4·110	8·483	11·136
		4	1·850	4·189	8·621	11·253
		8	1·865	4·225	8·667	11·280
	45	2	1·818	5·415	8·470	11·985
		4	1·839	5·501	8·548	12·016
		8	1·848	5·537	8·565	12·003

generic presentation of the vibration results, the effects of various design parameters, such as plate thickness, skew angle, facing fibre orientation, and boundary conditions, on the natural frequencies may be readily examined.

This paper also features a large amount of new frequency data for such a class of skew sandwich plates. These data should be useful to engineers and researchers working in the area of composite plates.

REFERENCES

1. G. R. MONFORTON and I. M. IBRAHIM 1975 *International Journal of Mechanical Sciences* **17**, 227–238. Analysis of sandwich plates with unbalanced cross-ply faces.
2. G. R. MONFORTON and I. M. IBRAHIM 1977 *International Journal of Mechanical Sciences* **19**, 335–343. Modified stiffness formulation of unbalanced anisotropic sandwich plates.
3. I. M. IBRAHIM, A. FARAH and M. N. F. RIZK 1981 *Journal of Engineering Mechanics ASCE* **107**, 405–418. Dynamic analysis of unbalanced anisotropic sandwich plates.
4. H. H. KANEMATU and Y. HIRANO 1988 *Composite Structures* **10**, 145–163. Bending and vibration of CFRP-faced rectangular sandwich plates.
5. K. M. LIEW, C. M. WANG, Y. XIANG and S. KITIPORNCHAI 1998 *Vibration of Mindlin Plates: Programming the p-version Ritz Method*. Oxford: Elsevier.
6. K. M. LIEW, Y. XIANG, C. M. WANG and S. KITIPORNCHAI 1998. *Journal of Sound and Vibration* **168**, 36–69. Vibration of thick skew plates based on Mindlin shear deformation plate theory.
7. *ABAQUS User's Manual*, Version 5.7. Habitt, Karlsson & Sorensen, Inc.
8. B. T. SMITH, J. M. BOYLE, B. S. GARBOW, Y. IKEBE, V. C. KLEMA and C. B. MOLAR 1974. *Matrix Eigensystem Routines—EISPACK Guide*. New York: Springer-Verlag.
9. S. WANG 1997 *Computers and Structures* **63**, 525–538. Free vibration analysis of skew fibre-reinforced composite laminates based on first-order shear deformation plate theory.

APPENDIX A

The elements of the stiffness matrix $[K]$ are given by

$$K_{ij}^{cc} = \frac{8K_s}{\tau^2}\int_{-1}^{1}\int_{-1}^{1}\Bigg[(\tan^2\beta A_{44}^{(s)} - 2\tan\beta A_{45}^{(s)} + A_{55}^{(s)} + G_x^c t_c + \tan^2\beta G_y^c t_c)\frac{\partial\chi_i^w}{\partial\xi}\frac{\partial\chi_j^w}{\partial\xi}$$

$$+\frac{\sec^2\beta}{\alpha^2}(A_{44}^{(s)} + G_y^c t_c)\frac{\partial\chi_i^w}{\partial\eta}\frac{\partial\chi_j^w}{\partial\eta} + \frac{\sec\beta}{\alpha}(-\tan\beta A_{44}^{(s)} + A_{45}^{(s)} - \tan\beta G_y^c t_c)$$

$$\times\left(\frac{\partial\chi_i^w}{\partial\xi}\frac{\partial\chi_j^w}{\partial\eta} + \frac{\partial\chi_i^w}{\partial\eta}\frac{\partial\chi_j^w}{\partial\xi}\right)\Bigg]\mathrm{d}\xi\,\mathrm{d}\eta,$$

$$K_{ij}^{cd} = \frac{4K_s}{\tau}\int_{-1}^{1}\int_{-1}^{1}\Bigg[(-\sin\beta\tan\beta A_{44}^{(s)} + 2\sin\beta A_{45}^{(s)} - \cos\beta A_{55}^{(s)})\frac{\partial\chi_i^w}{\partial\xi}\chi_j^d$$

$$+\left(\frac{\tan\beta A_{44}^{(s)}}{\alpha} - \frac{A_{45}^{(s)}}{\alpha}\right)\frac{\partial\chi_i^w}{\partial\eta}\chi_j^d\Bigg]\mathrm{d}\xi\,\mathrm{d}\eta,$$

$$K_{ij}^{ce} = \frac{4K_s}{\tau}\int_{-1}^{1}\int_{-1}^{1}\left[(\tan\beta A_{44}^{(s)} - A_{45}^{(s)})\frac{\partial\chi_i^w}{\partial\xi}\chi_j^e - \frac{\sec\beta A_{44}^{(s)}}{\alpha}\frac{\partial\chi_i^w}{\partial\eta}\chi_j^e\right]\mathrm{d}\xi\,\mathrm{d}\eta,$$

$$K_{ij}^{cf} = \frac{4t_c K_s}{\tau}\int_{-1}^{1}\int_{-1}^{1}\left[\frac{\tan\beta G_y^c}{\alpha}\frac{\partial\chi_i^w}{\partial\eta}\chi_j^f - (\cos\beta G_x^c + \sin\beta\tan\beta G_y^c)\frac{\partial\chi_i^w}{\partial\xi}\chi_j^f\right]\mathrm{d}\xi\,\mathrm{d}\eta,$$

$$K_{ij}^{cg} = \frac{4t_c K_s}{\tau}\int_{-1}^{1}\int_{-1}^{1}\left[\tan\beta G_y^c\frac{\partial\chi_i^w}{\partial\xi}\chi_j^g - \frac{\sec\beta G_y^c}{\alpha}\frac{\partial\chi_i^w}{\partial\eta}\chi_j^g\right]\mathrm{d}\xi\,\mathrm{d}\eta,$$

$$\begin{aligned}K_{ij}^{dd} = 2\int_{-1}^{1}\int_{-1}^{1}\Bigg\{&\Bigg[\frac{4}{a^2}(\cos^2\beta D_{11} + 2\sin^2\beta D_{12} - 4\sin\beta\cos\beta D_{16} + \sin^2\beta\tan^2\beta D_{22}\\
&- 4\sin^2\beta\tan\beta D_{26} + 4\sin^2\beta D_{66}) + \lambda_c^2(\cos^2\beta A_{11}^{(m)} + 2\sin^2\beta A_{12}^{(m)}\\
&- 4\sin\beta\cos\beta A_{16}^{(m)} + \sin^2\beta\tan^2\beta A_{22}^{(m)} - 4\sin^2\beta\tan\beta A_{26}^{(m)} + 4\sin^2\beta A_{66}^{(m)})\\
&- \frac{8\lambda_c}{a}(\cos^2\beta E_{11} + 2\sin^2\beta E_{12} - 4\sin\beta\cos\beta E_{16} + \sin^2\beta\tan^2\beta E_{22}\\
&- 4\sin^2\beta\tan\beta E_{26} + 4\sin^2\beta E_{66})\Bigg]\frac{\partial\chi_i^d}{\partial\xi}\frac{\partial\chi_j^d}{\partial\xi} + \Bigg[\frac{4}{b^2}(\tan^2\beta D_{22} - 2\tan\beta D_{26} + D_{66})\\
&+ \frac{\lambda_c^2}{\alpha^2}(\tan^2\beta A_{22}^{(m)} - 2\tan\beta A_{26}^{(m)} + A_{66}^{(m)}) - \frac{8\lambda_c}{b\alpha}(\tan^2\beta E_{22} - 2\tan\beta E_{26} + E_{66})\Bigg]\\
&\times\frac{\partial\chi_i^d}{\partial\eta}\frac{\partial\chi_j^d}{\partial\eta} + \Bigg[\frac{4}{ab}(-\sin\beta D_{12} + \cos\beta D_{16} - \sin\beta\tan^2\beta D_{22}\\
&+ 3\sin\beta\tan\beta D_{26} - 2\sin\beta D_{66}) + \frac{\lambda_c^2}{\alpha}(-\sin\beta A_{12}^{(m)} + \cos\beta A_{16}^{(m)}\\
&- \sin\beta\tan^2\beta A_{22}^{(m)} + 3\sin\beta\tan\beta A_{26}^{(m)} - 2\sin\beta A_{66}^{(m)}) - \frac{8\lambda_c}{b}\\
&\times(-\sin\beta E_{12} + \cos\beta E_{16} - \sin\beta\tan^2\beta E_{22} + 3\sin\beta\tan\beta E_{26} - 2\sin\beta E_{66})\Bigg]\\
&\times\left(\frac{\partial\chi_i^d}{\partial\xi}\frac{\partial\chi_j^d}{\partial\eta} + \frac{\partial\chi_i^d}{\partial\eta}\frac{\partial\chi_j^d}{\partial\xi}\right) + K_s(\sin^2\beta A_{44}^{(s)} - 2\sin\beta\cos\beta A_{45}^{(s)} + \cos^2\beta A_{55}^{(s)})\chi_i^d\chi_j^d\Bigg\}\mathrm{d}\xi\,\mathrm{d}\eta,\end{aligned}$$

$$\begin{aligned}K_{ij}^{de} = 2\int_{-1}^{1}\int_{-1}^{1}\Bigg\{&\Bigg[\frac{4}{a^2}(-\sin\beta D_{12} + \cos\beta D_{16} - \sin\beta\tan^2\beta D_{22} + 3\sin\beta\tan\beta D_{26}\\
&- 2\sin\beta D_{66}) + \lambda_c^2(-\sin\beta A_{12}^{(m)} + \cos\beta A_{16}^{(m)} - \sin\beta\tan^2\beta A_{22}^{(m)}\\
&+ 3\sin\beta\tan\beta A_{26}^{(m)} - 2\sin\beta A_{66}^{(m)}) + \frac{8\lambda_c}{a}(-\sin\beta E_{12} + \cos\beta E_{16}\end{aligned}$$

$$- \sin\beta\tan^2\beta E_{22} + 3\sin\beta\tan\beta E_{26} - 2\sin\beta E_{66})\Big]\frac{\partial\chi_i^d}{\partial\xi}\frac{\partial\chi_j^e}{\partial\xi}$$

$$+\Big[\frac{4}{ab}(D_{12} + \tan^2\beta D_{22} - 2\tan\beta D_{26}) + \frac{\lambda_c^2}{\alpha}(A_{12}^{(m)} + \tan^2\beta A_{22}^{(m)} - 2\tan\beta A_{26}^{(m)})$$

$$-\frac{8\lambda_c}{b}(E_{12} + \tan^2\beta E_{22} - 2\tan\beta E_{26})\Big]\frac{\partial\chi_i^d}{\partial\xi}\frac{\partial\chi_j^e}{\partial\eta}$$

$$+\Big[\frac{4}{ab}(\tan^2\beta D_{22} - 2\tan\beta D_{26} + D_{66}) + \frac{\lambda_c^2}{\alpha}(\tan^2\beta A_{22}^{(m)} - 2\tan\beta A_{26}^{(m)} + A_{66}^{(m)})$$

$$-\frac{8\lambda_c}{b}(\tan^2\beta E_{22} - 2\tan\beta E_{26} + E_{66})\Big]\frac{\partial\chi_i^d}{\partial\eta}\frac{\partial\chi_j^e}{\partial\xi} + \Big[\frac{4}{b^2}(-\tan\beta\sec\beta D_{22} + \sec\beta D_{26})$$

$$+\frac{\lambda_c^2}{\alpha^2}(-\tan\beta\sec\beta A_{22}^{(m)} + \sec\beta A_{26}^{(m)}) - \frac{8\lambda_c}{\alpha b}(-\tan\beta\sec\beta E_{22} + \sec\beta E_{26})\Big]$$

$$\times\frac{\partial\chi_i^d}{\partial\eta}\frac{\partial\chi_j^e}{\partial\eta} + K_s(\cos\beta A_{45}^{(s)} - \sin\beta A_{44}^{(s)})\chi_i^d\chi_j^e\Big\}\,\mathrm{d}\xi\,\mathrm{d}\eta,$$

$$K_{ij}^{df} = 2\int_{-1}^{1}\int_{-1}^{1}\Big\{\Big[-\lambda_c^2(\cos^2\beta A_{11}^{(m)} + 2\sin^2\beta A_{12}^{(m)} - 4\sin\beta\cos\beta A_{16}^{(m)} + \tan^2\beta\sin^2\beta A_{22}^{(m)}$$

$$-4\sin^2\beta\tan\beta A_{26}^{(m)} + 4\sin^2\beta A_{66}^{(m)}) + \frac{4\alpha_c}{a}(\cos^2\beta E_{11} + 2\sin^2\beta E_{12}$$

$$-4\sin\beta\cos\beta E_{16} + \tan^2\beta\sin^2\beta E_{22} - 4\sin^2\beta\tan\beta E_{26}$$

$$+4\sin^2\beta E_{66})\Big]\frac{\partial\chi_i^d}{\partial\xi}\frac{\partial\chi_j^f}{\partial\xi} + \Big[-\frac{\lambda_c^2}{\alpha^2}(\tan^2\beta A_{22}^{(m)} - 2\tan\beta A_{26}^{(m)} + A_{66}^{(m)})$$

$$+\frac{4\lambda_c}{\alpha b}(\tan^2\beta E_{22} - 2\tan\beta E_{26} + E_{66})\Big]\frac{\partial\chi_i^d}{\partial\eta}\frac{\partial\chi_j^f}{\partial\eta} + \Big[-\frac{\lambda_c^2}{\alpha}(-\sin\beta A_{12}^{(m)}$$

$$+\cos\beta A_{16}^{(m)} - \sin\beta\tan^2\beta A_{22}^{(m)} + 3\sin\beta\tan\beta A_{26}^{(m)} - 2\sin\beta A_{66}^{(m)})$$

$$+\frac{4\lambda_c}{b}(-\sin\beta E_{12} + \cos\beta E_{16} - \sin\beta\tan^2\beta E_{22} + 3\sin\beta\tan\beta E_{26}$$

$$-2\sin\beta E_{66})\Big]\Big(\frac{\partial\chi_i^d}{\partial\xi}\frac{\partial\chi_j^f}{\partial\eta} + \frac{\partial\chi_i^d}{\partial\eta}\frac{\partial\chi_j^f}{\partial\xi}\Big)\Big\}\,\mathrm{d}\xi\,\mathrm{d}\eta,$$

$$K_{ij}^{dg} = 2\int_{-1}^{1}\int_{-1}^{1}\Bigg\{\Bigg[-\lambda_c^2(-\sin\beta A_{12}^{(m)} + \cos\beta A_{16}^{(m)} - \sin\beta\tan^2\beta A_{22}^{(m)}$$

$$+ 3\sin\beta\tan\beta A_{26}^{(m)} - 2\sin\beta A_{66}^{(m)}) + \frac{4\lambda_c}{a}(-\sin\beta E_{12} + \cos\beta E_{16}$$

$$-\sin\beta\tan^2\beta E_{22} + 3\sin\beta\tan\beta E_{26} - 2\sin\beta E_{66})\Bigg]\frac{\partial\chi_i^d}{\partial\xi}\frac{\partial\chi_j^g}{\partial\xi}$$

$$+\Bigg[-\frac{\lambda_c^2}{\alpha}(A_{12}^{(m)} + \tan^2\beta A_{22}^{(m)} - 2\tan\beta A_{26}^{(m)}) + \frac{4\lambda_c}{b}(E_{12} + \tan^2\beta E_{22}$$

$$-2\tan\beta E_{26})\Bigg]\frac{\partial\chi_i^d}{\partial\xi}\frac{\partial\chi_j^g}{\partial\eta} + \Bigg[-\frac{\lambda_c^2}{\alpha}(\tan^2\beta A_{22}^{(m)} - 2\tan\beta A_{26}^{(m)} + A_{66}^{(m)})$$

$$+\frac{4\lambda_c}{b}(\tan^2\beta E_{22} - 2\tan\beta E_{26} + E_{66})\Bigg]\frac{\partial\chi_i^d}{\partial\eta}\frac{\partial\chi_j^g}{\partial\xi} + \Bigg[-\frac{\lambda_c^2}{\alpha^2}(-\tan\beta\sec\beta A_{22}^{(m)}$$

$$+\sec\beta A_{26}^{(m)}) + \frac{4\lambda_c}{\alpha b}(-\tan\beta\sec\beta E_{22} + \sec\beta E_{26})\Bigg]\frac{\partial\chi_i^d}{\partial\eta}\frac{\partial\chi_j^g}{\partial\eta}\Bigg\}\,\mathrm{d}\xi\,\mathrm{d}\eta,$$

$$K_{ij}^{ee} = 2\int_{-1}^{1}\int_{-1}^{1}\Bigg\{\Bigg[\frac{4}{a^2}(\tan^2\beta D_{22} - 2\tan\beta D_{26} + D_{66}) + \lambda_c^2(\tan^2\beta A_{22}^{(m)} - 2\tan\beta A_{26}^{(m)}$$

$$+A_{66}^{(m)}) - \frac{8\lambda_c}{a}(\tan^2\beta E_{22} - 2\tan\beta E_{26} + E_{66})\Bigg]\frac{\partial\chi_I^e}{\partial\xi}\frac{\partial\chi_j^e}{\partial\xi}$$

$$+\left(\frac{4\sec^2\beta}{b^2}D_{22} + \frac{\lambda_c^2\sec^2\beta}{\alpha^2}A_{22}^{(m)} - \frac{8\lambda_c\sec^2\beta}{\alpha b}E_{22}\right)\frac{\partial\chi_i^e}{\partial\eta}\frac{\partial\chi_j^e}{\partial\eta}$$

$$+\Bigg[\frac{4}{ab}(-\tan\beta\sec\beta D_{22} + \sec\beta D_{26}) + \frac{\lambda_c^2}{\alpha}(-\tan\beta\sec\beta A_{22}^{(m)} + \sec\beta A_{26}^{(m)})$$

$$-\frac{8\lambda_c}{b}(-\tan\beta\sec\beta E_{22} + \sec\beta E_{26})\Bigg]\left(\frac{\partial\chi_i^e}{\partial\xi}\frac{\partial\chi_j^e}{\partial\eta} + \frac{\partial\chi_i^e}{\partial\eta}\frac{\partial\chi_j^e}{\partial\xi}\right) + \mathrm{K}_s A_{44}^{(s)}\chi_i^e\chi_j^e\Bigg\}\,\mathrm{d}\xi\,\mathrm{d}\eta,$$

$$K_{ij}^{ef} = 2\int_{-1}^{1}\int_{-1}^{1}\Bigg\{\Bigg[-\lambda_c^2(-\sin\beta A_{12}^{(m)} + \cos\beta A_{16}^{(m)} - \sin\beta\tan^2\beta A_{22}^{(m)}$$

$$+ 3\sin\beta\tan\beta A_{26}^{(m)} - 2\sin\beta A_{66}^{(m)}) + \frac{4\lambda_c}{a}(-\sin\beta E_{12} + \cos\beta E_{16}$$

$$-\sin\beta\tan^2\beta E_{22} + 3\sin\beta\tan\beta E_{26} - 2\sin\beta E_{66})\Bigg]\frac{\partial\chi_i^e}{\partial\xi}\frac{\partial\chi_j^f}{\partial\xi}$$

$$+\left[-\frac{\lambda_c^2}{\alpha}(A_{12}^{(m)}+\tan^2\beta A_{22}^{(m)}-2\tan\beta A_{26}^{(m)})+\frac{4\lambda_c}{b}(E_{12}+\tan^2\beta E_{22}\right.$$

$$\left.-2\tan\beta E_{26})\right]\frac{\partial\chi_i^e}{\partial\eta}\frac{\partial\chi_j^f}{\partial\xi}+\left[-\frac{\lambda_c^2}{\alpha}(\tan^2\beta A_{22}^{(m)}-2\tan\beta A_{26}^{(m)}+A_{66}^{(m)})\right.$$

$$\left.+\frac{4\lambda_c}{b}(\tan^2\beta E_{22}-2\tan\beta E_{26}+E_{66})\right]\frac{\partial\chi_i^e}{\partial\xi}\frac{\partial\chi_j^f}{\partial\eta}+\left[-\frac{\lambda_c^2}{\alpha^2}(-\tan\beta\sec\beta A_{22}^{(m)}\right.$$

$$\left.+\sec\beta A_{26}^{(m)})+\frac{4\lambda_c}{\alpha b}(-\tan\beta\sec\beta E_{22}+\sec\beta E_{26})\right]\frac{\partial\chi_i^e}{\partial\eta}\frac{\partial\chi_j^f}{\partial\eta}\Bigg\}\,\mathrm{d}\xi\,\mathrm{d}\eta,$$

$$K_{ij}^{eg}=2\int_{-1}^{1}\int_{-1}^{1}\Bigg\{\Bigg[-\lambda_c^2(\tan^2\beta A_{22}^{(m)}-2\tan\beta A_{26}^{(m)}+A_{66}^{(m)})+\frac{4\lambda_c}{a}(\tan^2\beta E_{22}$$

$$-2\tan\beta E_{26}+E_{66})\Bigg]\frac{\partial\chi_i^e}{\partial\xi}\frac{\partial\chi_j^g}{\partial\xi}+\left(-\frac{\lambda_c^2\sec^2\beta}{\alpha^2}A_{22}^{(m)}+\frac{4\lambda_c\sec^2\beta}{\alpha b}E_{22}\right)\frac{\partial\chi_i^e}{\partial\eta}\frac{\partial\chi_j^g}{\partial\eta}$$

$$+\left[-\frac{\lambda_c^2}{\alpha}\left(-\tan\beta\sec\beta A_{22}^{(m)}+\sec\beta A_{26}^{(m)}\right)+\frac{4\lambda_c}{b}(-\tan\beta\sec\beta E_{22}\right.$$

$$\left.+\sec\beta E_{26})\right]\left(\frac{\partial\chi_i^e}{\partial\xi}\frac{\partial\chi_j^g}{\partial\eta}+\frac{\partial\chi_i^e}{\partial\eta}\frac{\partial\chi_j^g}{\partial\xi}\right)\Bigg\}\,\mathrm{d}\xi\,\mathrm{d}\eta,$$

$$K_{ij}^{ff}=2\int_{-1}^{1}\int_{-1}^{1}\Bigg[\lambda_c^2(\cos^2\beta A_{11}^{(m)}+2\sin^2\beta A_{12}^{(m)}-4\sin\beta\cos\beta A_{16}^{(m)}+\tan^2\beta\sin^2\beta A_{22}^{(m)}$$

$$-4\sin^2\beta\tan\beta A_{26}^{(m)}+4\sin^2\beta A_{66}^{(m)})\frac{\partial\chi_i^f}{\partial\xi}\frac{\partial\chi_j^f}{\partial\xi}+\frac{\lambda_c^2}{\alpha^2}(\tan^2\beta A_{22}^{(m)}$$

$$-2\tan\beta A_{26}^{(m)}+A_{66}^{(m)})\frac{\partial\chi_i^f}{\partial\eta}\frac{\partial\chi_j^f}{\partial\eta}+\frac{\lambda_c^2}{\alpha}(-\sin\beta A_{12}^{(m)}+\cos\beta A_{16}^{(m)}$$

$$-\sin\beta\tan^2\beta A_{22}^{(m)}+3\sin\beta\tan\beta A_{26}^{(m)}-2\sin\beta A_{66}^{(m)})\left(\frac{\partial\chi_i^f}{\partial\xi}\frac{\partial\chi_j^f}{\partial\eta}+\frac{\partial\chi_i^f}{\partial\eta}\frac{\partial\chi_j^f}{\partial\xi}\right)$$

$$+t_cK_s(\cos^2\beta G_x^c+\sin^2\beta G_y^c)\chi_i^f\chi_j^f\Bigg]\,\mathrm{d}\xi\,\mathrm{d}\eta,$$

$$K_{ij}^{fg}=2\int_{-1}^{1}\int_{-1}^{1}\Bigg[\lambda_c^2(-\sin\beta A_{12}^{(m)}+\cos\beta A_{16}^{(m)}-\sin\beta\tan^2\beta A_{22}^{(m)}+3\sin\beta\tan\beta A_{26}^{(m)}$$

$$-2\sin\beta A_{66}^{(m)})\frac{\partial\chi_i^f}{\partial\xi}\frac{\partial\chi_j^g}{\partial\xi}+\frac{\lambda_c^2}{\alpha}(A_{12}^{(m)}+\tan^2\beta A_{22}^{(m)}-2\tan\beta A_{26}^{(m)})\frac{\partial\chi_i^f}{\partial\xi}\frac{\partial\chi_j^g}{\partial\eta}$$

$$+\frac{\lambda_c^2}{\alpha}(\tan^2\beta A_{22}^{(m)} - 2\tan\beta A_{26}^{(m)} + A_{66}^{(m)})\frac{\partial\chi_i^f}{\partial\eta}\frac{\partial\chi_j^g}{\partial\xi} + \frac{\lambda_c^2}{\alpha^2}(-\tan\beta\sec\beta A_{22}^{(m)}$$

$$+\sec\beta A_{26}^{(m)})\frac{\partial\chi_i^f}{\partial\eta}\frac{\partial\chi_j^g}{\partial\eta} - \sin\beta t_c G_y^c \chi_i^f \chi_j^g\Bigg]\mathrm{d}\xi\,\mathrm{d}\eta,$$

$$K_{ij}^{gg} = 2\int_{-1}^{1}\int_{-1}^{1}\Bigg[\lambda_c^2\left(\tan^2\beta A_{22}^{(m)} - 2\tan\beta A_{26}^{(m)} + A_{66}^{(m)}\right)\frac{\partial\chi_i^g}{\partial\xi}\frac{\partial\chi_j^g}{\partial\xi}$$

$$+\frac{\lambda_c^2\sec^2\beta A_{22}^{(m)}}{\alpha^2}\frac{\partial\chi_i^g}{\partial\eta}\frac{\partial\chi_j^g}{\partial\eta} + \frac{\lambda_c^2}{\alpha}(-\tan\beta\sec\beta A_{22}^{(m)} + \sec\beta A_{26}^{(m)})$$

$$\times\left(\frac{\partial\chi_i^g}{\partial\xi}\frac{\partial\chi_j^g}{\partial\eta} + \frac{\partial\chi_i^g}{\partial\eta}\frac{\partial\chi_j^g}{\partial\xi}\right) + K_s t_c G_y^c \chi_i^g \chi_j^g\Bigg]\mathrm{d}\xi\,\mathrm{d}\eta.$$

The elements of the mass matrix $[M]$ are given by

$$M_{ij}^{cc} = \frac{2S_o(\mu_1\lambda_1 + \mu_2\lambda_2 + \lambda_c)}{a^2\beta^2}\int_{-1}^{1}\int_{-1}^{1}\chi_i^c\chi_j^c\,\mathrm{d}\xi\,\mathrm{d}\eta,$$

$$M_{ij}^{cd} = 0, \quad M_{ij}^{ce} = 0, \quad M_{ij}^{cf} = 0, \quad M_{ij}^{cg} = 0,$$

$$M_{ij}^{dd} = \frac{2S_o(\mu_1\lambda_1^3 + \mu_2\lambda_2^3)}{3a^2}\int_{-1}^{1}\int_{-1}^{1}\chi_i^d\chi_j^d\,\mathrm{d}\xi\,\mathrm{d}\eta,$$

$$M_{ij}^{de} = -\frac{2S_o\sin\beta(\mu_1\lambda_1^3 + \mu_2\lambda_2^3)}{3a^2}\int_{-1}^{1}\int_{-1}^{1}\chi_i^d\chi_j^e\,\mathrm{d}\xi\,\mathrm{d}\eta,$$

$$M_{ij}^{df} = \frac{S_o\lambda_c(\mu_1\lambda_1^2 + \mu_2\lambda_2^2)}{2a^2}\int_{-1}^{1}\int_{-1}^{1}\chi_i^d\chi_j^f\,\mathrm{d}\xi\,\mathrm{d}\eta,$$

$$M_{ij}^{dg} = -\frac{S_o\sin\beta\lambda_c(\mu_1\lambda_1^2 + \mu_2\lambda_2^2)}{2a^2}\int_{-1}^{1}\int_{-1}^{1}\chi_i^d\chi_j^g\,\mathrm{d}\xi\,\mathrm{d}\eta,$$

$$M_{ij}^{ee} = \frac{2S_o(\mu_1\lambda_1^3 + \mu_2\lambda_2^3)}{3a^2}\int_{-1}^{1}\int_{-1}^{1}\chi_i^e\chi_j^e\,\mathrm{d}\xi\,\mathrm{d}\eta,$$

$$M_{ij}^{ef} = -\frac{S_o\sin\beta\lambda_c(\mu_1\lambda_1^2 + \mu_2\lambda_2^2)}{2a^2}\int_{-1}^{1}\int_{-1}^{1}\chi_i^e\chi_j^f\,\mathrm{d}\xi\,\mathrm{d}\eta,$$

$$M_{ij}^{eg} = \frac{S_o\lambda_c(\mu_1\lambda_1^2 + \mu_2\lambda_2^2)}{2a^2}\int_{-1}^{1}\int_{-1}^{1}\chi_i^e\chi_j^g\,\mathrm{d}\xi\,\mathrm{d}\eta,$$

$$M_{ij}^{ff} = \frac{S_o\lambda_c^2(3\mu_1\lambda_1 + 3\mu_2\lambda_2 + \lambda_c)}{6a^2}\int_{-1}^{1}\int_{-1}^{1}\chi_i^f\chi_j^f\,\mathrm{d}\xi\,\mathrm{d}\eta,$$

$$M_{ij}^{fg} = -\frac{S_o \sin\beta\lambda_c^2(3\mu_1\lambda_1 + 3\mu_2\lambda_2 + \lambda_c)}{6a^2}\int_{-1}^{1}\int_{-1}^{1}\chi_i^f\chi_j^g\,\mathrm{d}\xi\,\mathrm{d}\eta,$$

$$M_{ij}^{gg} = \frac{S_o\lambda_c^2(3\mu_1\lambda_1 + 3\mu_2\lambda_2 + \lambda_c)}{6a^2}\int_{-1}^{1}\int_{-1}^{1}\chi_i^g\chi_j^g\,\mathrm{d}\xi\,\mathrm{d}\eta,$$

where $i = 1, 2, \ldots, N$, $j = 1, 2, \ldots, N$ and

$$\alpha = \frac{b}{a}, \quad \tau = \frac{a}{h}, \quad \mu_f = \frac{\rho_f}{\rho_c}, \quad \lambda_f = \frac{t_f}{a}, \quad \lambda_c = \frac{t_c}{a}, \quad S_o = E_{11}a^3 \times 10^{-4}.$$